Nanofabrication Advances for High Efficiency Critical-Angle Transmission Gratings

Alexander R. Bruccoleri[a], Dong Guan[a], Ralf K. Heilmann[a], Steve Vargo[b], Frank DiPiazza[c] and Mark L. Schattenburg[a]

[a]Space Nanotechnology Laboratory, MIT Kavli Institute for Astrophysics and Space Research, Massachusetts Institute of Technology, Cambridge, MA 02139, USA;
[b]SPTS Technologies, Inc., 1150 Ringwood Ct., San Jose, CA 95131, USA;
[c]Silicon Resources LLC, 1158 Blue Heron, Highland, MI 48357, USA

ABSTRACT

We report several break-through nanofabrication developments enabling high efficiency and high resolving power spectrometers in the soft x-ray band. The device is the critical-angle transmission (CAT) grating, which combines the low mass and relaxed alignment tolerances of a transmission grating with the high broad-band efficiency and high diffraction orders of a blazed reflection grating. Past work successfully demonstrated the CAT grating concept; however, the open-area fraction was often less than 20% whilst more than 50% is desired. This presents numerous nanofabrication challenges including a requirement for a freestanding silicon membrane of ultra high-aspect ratio bars at a period of 200 nanometers with minimal cross support blockage. Furthermore, the sidewalls must be smooth to a few nanometers to efficiently reflect soft x-rays. We have developed a complete nanofabrication process for creating freestanding CAT gratings via plasma-etching silicon wafers with a buried layer of SiO_2. This removable buried layer enables combining a record-performance plasma etch for the CAT grating with a millimeter-scale honeycomb structural support to create a large-area freestanding membrane. We have also developed a process for polishing sidewalls of plasma-etched ultra-high aspect ratio nanoscale silicon structures via potassium hydroxide (KOH). This process utilizes the anisotropic etch nature of single crystal silicon in KOH. We developed a novel alignment technique to align the CAT grating bars to the {111} planes of silicon within 0.2 degrees, which enables KOH to etch away sidewall roughness without destroying the structure, since the {111} planes etch approximately 100 times slower than the non-{111} planes. Preliminary results of a combined freestanding grating with polishing are presented to enable efficient diffraction of soft x-rays.

Keywords: Soft X-ray Diffraction, Blazed Grating, CAT Grating, DRIE, MEMS, KOH Polishing, Chemical Polishing, Interference Lithography, Pattern Transfer

1. INTRODUCTION

This paper presents progress on fabricating ultra-high aspect ratio freestanding gratings on the nanoscale for soft x-ray spectroscopy as described in detail by Bruccoleri.[1–3] Specifically, referred to as the critical-angle transmission (CAT) grating, it is targeted towards high-efficiency space-based x-ray spectrometers with high photon throughput due to its large size and high open-area fraction. The soft x-ray band with energies below 1 keV is of interest, covering the emission lines of nitrogen, oxygen, carbon, iron and neon.[4] In addition, other potential applications include ultraviolet filtration,[5] phase contrast imaging[6] and neutral mass spectroscopy.[7]

Conceptually, the CAT grating is a transmission grating that utilizes reflection, depicted in Figure 1. Incident x-rays reflect off the grating sidewalls at an angle θ_i, near or below θ_c, the critical angle for total external reflection. Diffraction takes place when the optical path length difference (OPLD) between parallel x-rays separated by one grating period, is an integer multiple of the x-ray wavelength. Precisely, the general grating equation is:

$$m\lambda = P\Big(sin(\theta_i) + sin(\beta_m)\Big), \tag{1}$$

Further author information: (Send correspondence to Dr. Alexander Bruccoleri)
E-mail: alexbruc@alum.mit.edu

Optics for EUV, X-Ray, and Gamma-Ray Astronomy VI, edited by Stephen L. O'Dell, Giovanni Pareschi, Proc. of SPIE Vol. 8861, 886119 · © 2013 SPIE
CCC code: 0277-786X/13/$18 · doi: 10.1117/12.2024357

where m is an integer designating the diffraction order, P is the grating period, β_m is the angle of the outgoing diffraction orders, θ_i is the angle of incidence and λ is the wavelength.

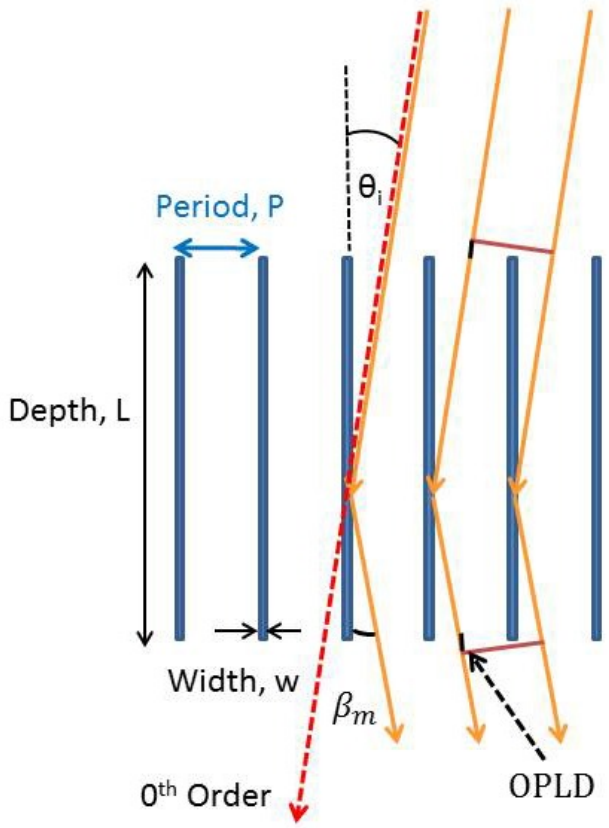

Figure 1: Conceptual drawing of x-ray diffraction and condition for total external reflection. (Not to scale.)

The x-rays enter the grating at a shallow graze angle relative to the grating bar sidewalls where they reflect with minimal absorption and maximum efficiency occurs when β_m is equal to θ_i. This blazing effect can significantly increase efficiency since the majority of the x-rays are directed into a small number of non-zero diffraction orders. The state-of-the-art in space-based phase-shifting x-ray transmission gratings are the gold-on-a-membrane gratings onboard the Chandra x-ray telescope. The gold bars absorb soft x-rays, reducing the gratings' efficiency.[8,9] The CAT grating avoids the majority of the absorption losses by reflecting the majority of the x-rays, increasing the soft x-ray efficiency by a factor up to five over the Chandra gratings.[10]

The x-rays must reflect at or below the critical angle for total external reflection θ_c, to be efficient, ($\theta_c \approx \sqrt{2\delta}$).[11] For silicon θ_c is a very shallow angle, $\approx 1.6°$, for λ of 1 nm, which leads to the required ultra-high aspect ratio for CAT grating bars. For efficient x-ray reflectivity the surfaces also have to be smooth. The efficiency of reflection is,

$$R(q) = R_o e^{-q^2\sigma^2}, \tag{2}$$

an exponential function of roughness, where R is the reflectivity, R_o is the reflectivity from a perfectly smooth surface, q is the momentum transfer of the reflection and σ is the roughness. The momentum transfer from a specular x-ray reflection is,

$$q = \frac{4\pi}{\lambda} n \sin\theta, \tag{3}$$

where θ is the angle of grazing incidence and n is the index of refraction of the material for the incident x-ray. In order to achieve $R/R_o \approx 90\%$ for a soft x-ray, λ of 1 nm, with a grazing incidence angle of 1.6°, the roughness needs to be on the order of 1 nm.

The specific geometry and dimensions for CAT gratings are set by the desired spectral band and telescope design. The current point-design has a 200-nm grating period, depth of 4 μm, bar width of 40 nm and surface roughness of the grating bars on the order of 1 nm. The goal is to provide $> 50\%$ diffraction efficiency for wavelengths between 2-7 nm for missions such as the Advanced X-ray Spectroscopy and Imaging Observatory (AXSIO) and the Square Meter Arcsecond Resolution X-ray Telescope (*SMART-X*).[12,13]

The fabrication processes developed by Bruccoleri et al. and summarized here successfully demonstrated gratings with the desired period and depth, with a net open-area fraction including all structural supports on the order of 30%, and spans of 31 mm on a side.[1] This is more than a factor of two improvement in aspect ratio of previous work on freestanding nanoscale gratings.[14] The fabrication process utilizes silicon-on-insulator (SOI) wafers and features integrated structural supports in the handle and device layers, referred to as Level 1 and Level 2 supports, respectively. The process utilizes deep reactive-ion etching (DRIE) for both the CAT grating and Level 1 supports in the SOI device and Level 2 supports in the handle layer, which allows for crystal lattice independent etching.[15] The main drawback of the process was the grating sidewalls were unpolished and likely not suitable for efficient reflection. To address the roughness a polishing process with potassium hydroxide (KOH) was developed by Bruccoleri et al. and summarized here.[3] This polishing process reduced the RMS roughness as measured with an AFM from 4 nm to 1 nm. Furthermore the width of the CAT grating bars were reduced from 100 nm to 70 nm. These features are over 30 times smaller than previously DRIE-KOH polished features published to date.[16,17] A combined process has been developed to create a freestanding grating with narrow and smooth sidewalls. The combined process is preliminary, and further refinement is required to improve the strength of the device.

2. FABRICATION METHODOLOGY

The fabrication methodology developed for freestanding gratings is based on integrated front and back side DRIE steps on SOI wafers (see Figure 2). A 4 μm-thick device layer is used for both the CAT grating and an integrated 5 μm-period cross support mesh designated "Level 1". A 500 μm handle layer serves as the large-area structural support designated "Level 2". The 500 nm-thick buried SiO_2 layer acts as an etch stop for both etches. The general fabrication procedure is as follows: After substrate preparation (1), the mask for the back side is patterned followed by front side masking (2). The front side is then deep-etched (3), filled and protected (4), flipped over and bonded to a carrier wafer. The back side is then deep-etched (5), the buried layer removed (6), and the sample is separated from the carrier, cleaned and critical-point dried to finish (7).

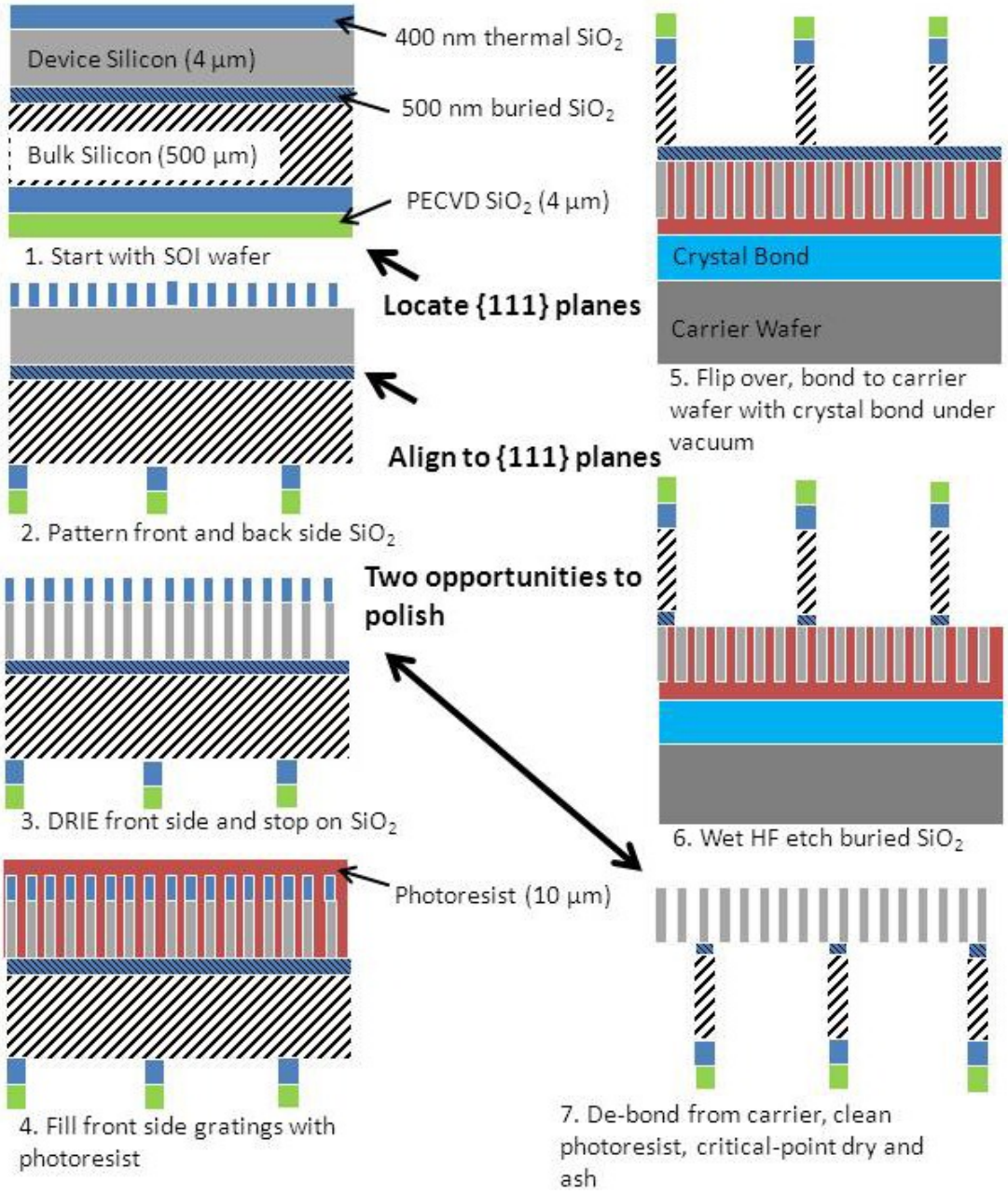

Figure 2: Process flow chart. The bold arrows are for future steps that integrate KOH polishing.

2.1 Freestanding Grating

The front side is masked with 400 nm of thermal SiO_2 and etched via the Bosch DRIE process in an STPS Pegasus tool as demonstrated in past work.[18] The 200 nm-period CAT grating is patterned via interference lithography (IL),[19] and transferred into the thermal SiO_2 layer via a tri-layer stack.[20] See Figure 3 for a scanning electron microscope (SEM) image of the 200 nm-period mask. The key step after deep etching the CAT grating is the photoresist-fill process of the CAT grating bars. The specific process is to apply two coatings of PFI-88A7 photoresist (Sumitomo Corporation) and one coat of AZ 4620 photoresist (AZ Electronic Materials). Both

photoresist are spin coated at at 3000 rpm, placed in vacuum ($\approx$ 0.25 atm) for outgassing and hotplate baked at 90° C for 60 seconds. The sample can be bonded to a carrier wafer via Crystalbond 555 (Structural Probe, Inc.) for back side etching since the CAT grating is filled and protected. See Figure 4 for SEM images of the deep-etch and the filled 4 μm deep grating.

The back side etch for the Level 2 structure is also performed with a Bosch process which stops on the same buried SiO_2 as the front side. The etch mask is 4 μm PECVD SiO_2 and 400 nm thermal SiO_2. The Level 2 structure is comprised of an array of 1 mm-wide hexagons with 100 μm-wide lines, spanning 31 mm on a side. See Figure 5 for a SEM image of the hexagon array. The buried SiO_2 is removed with a wet HF etch following the back side etch. The sample is removed from the carrier by immersing it in water at $\approx$ 80° C until the Crystalbond melts and the sample floats free. The photoresist filling is cleaned from the grating channels with two successive piranha cleans. The grating cannot be dried in air, since surface tension will pull the bars together. Instead the sample is kept submerged and critical-point dried to avoid the formation of liquid-air interfaces. Finally, the sample is placed in an asher (isotropic O_2 plasma) to clean any remaining organic material between the grating bars. The result is a fully integrated freestanding CAT grating structure (see Figure 6).

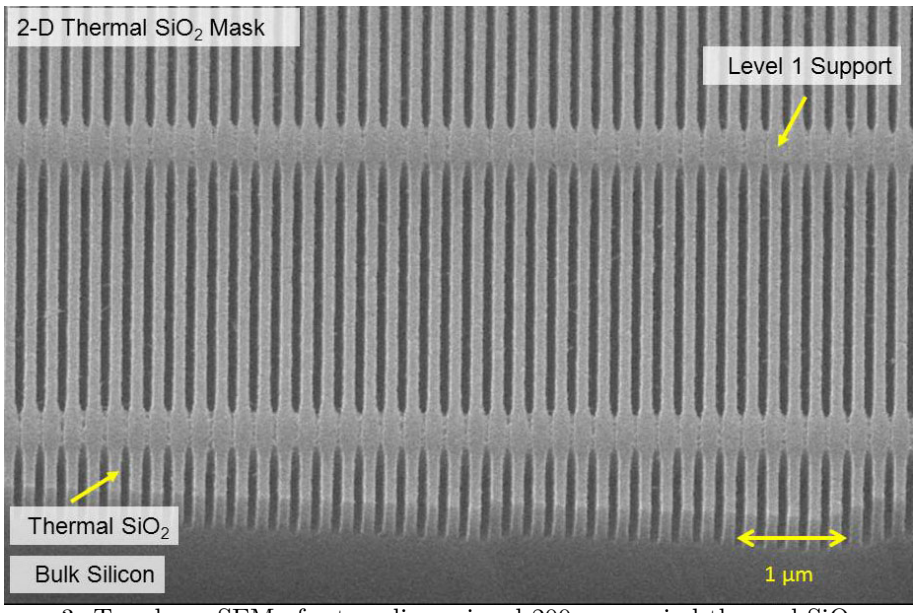

Figure 3: Top down SEM of a two-dimensional 200 nm-period thermal SiO_2 mask.

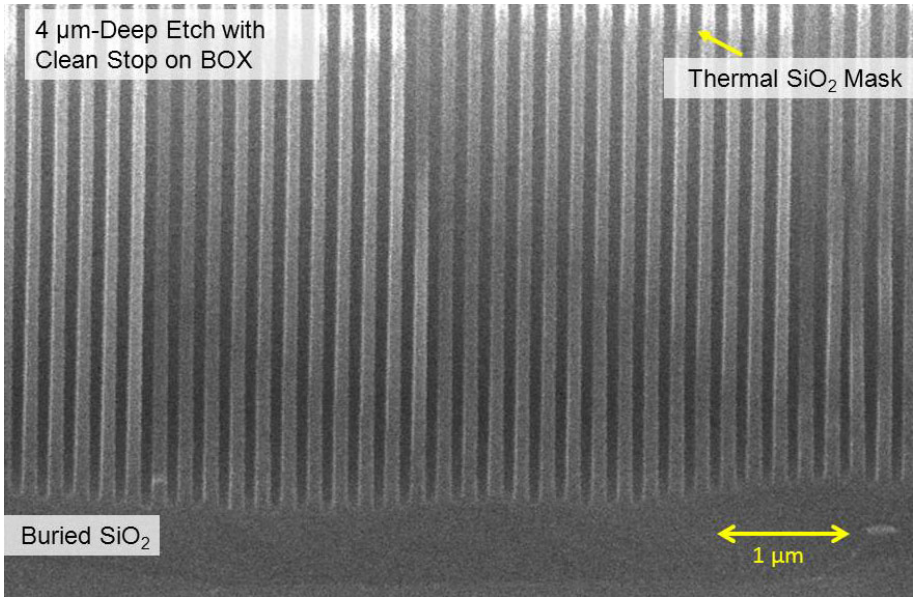

(a) Etched 4 μm deep and stopped on oxide

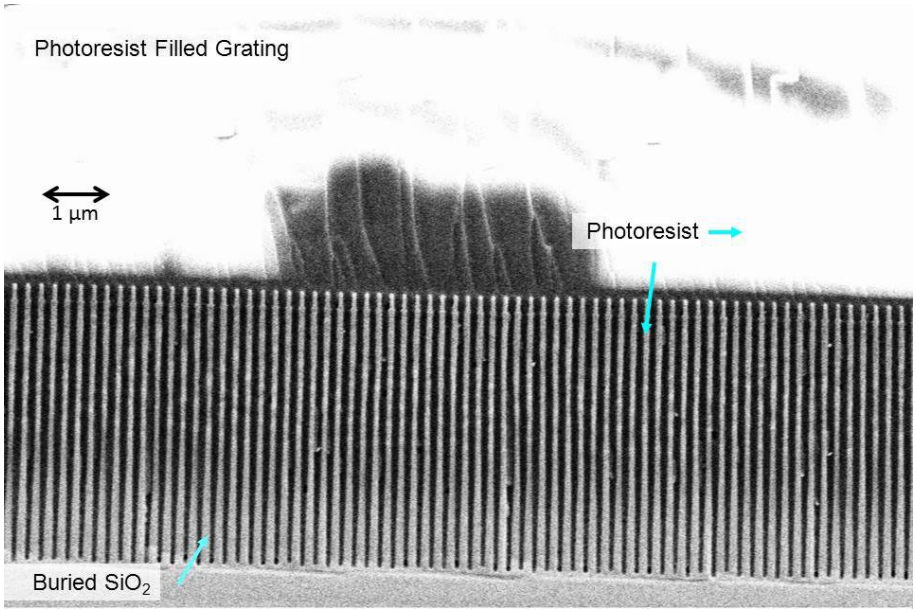

(b) Filled with photoresist

Figure 4: SEMs of cleaved 200 nm-period CAT gratings. Figures 4a and 4b are from different samples.

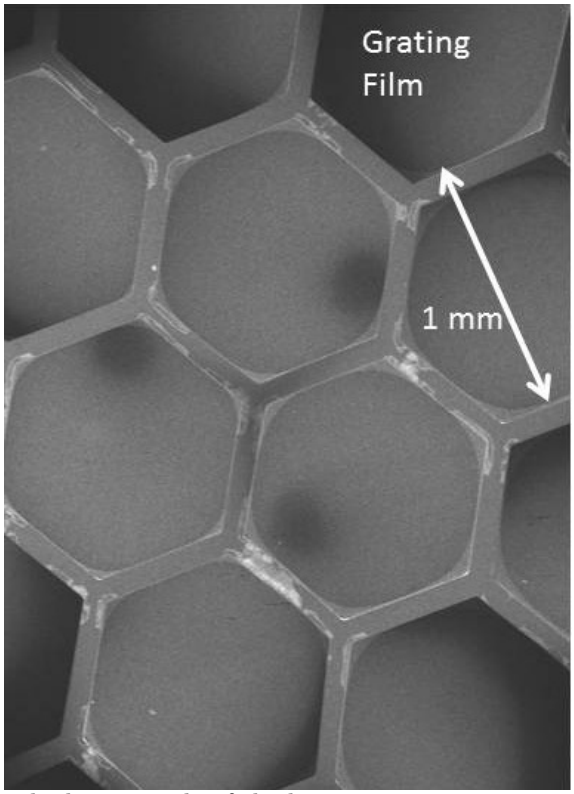

Figure 5: SEM from the bottom side of the hexagon support structure and grating film.

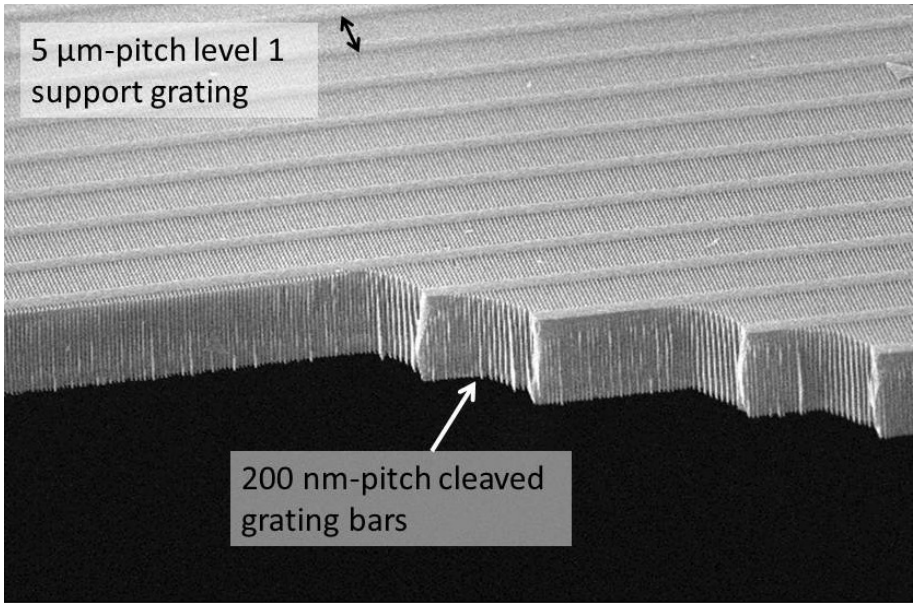

(a)

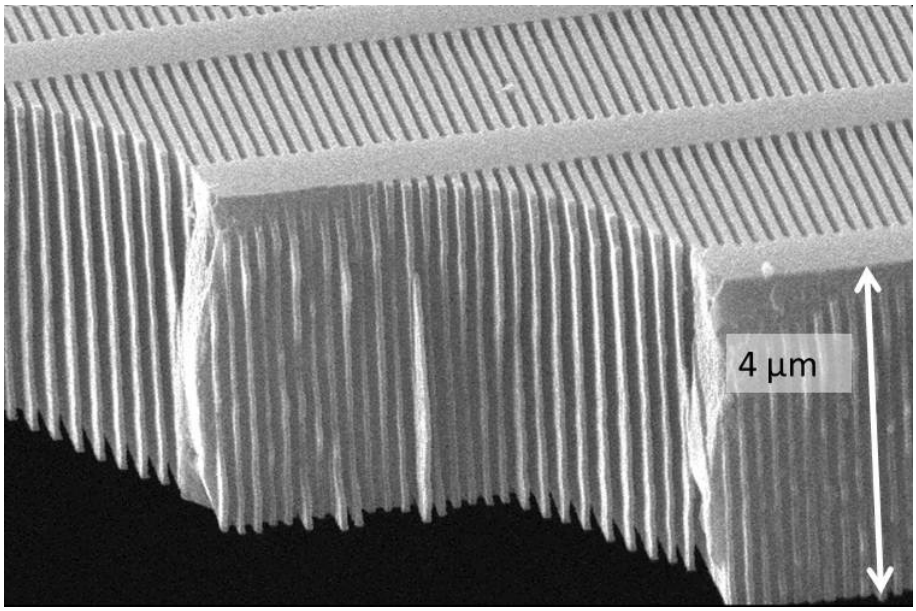

(b)

Figure 6

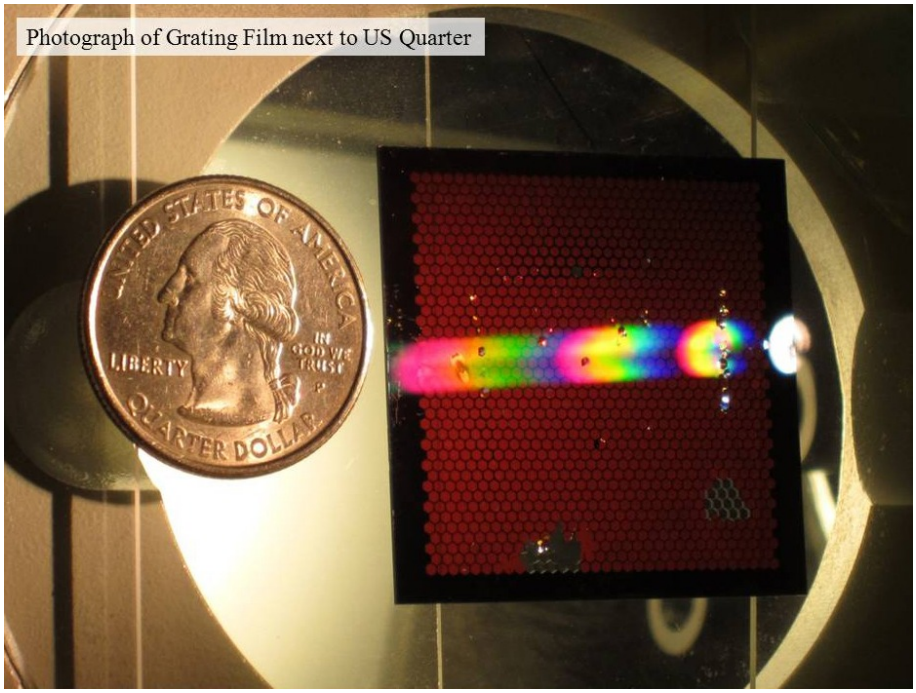

(c)

Figure 6: SEMs and photograph image of torn freestanding CAT grating film. (a) Zoomed out view of freestanding grating film. (b) Zoomed in view of freestanding grating film. (c) Photograph of CAT grating sample with US quarter for reference.

2.2 KOH Polishing

The process for a freestanding grating left sidewall roughness of approximately 4 nm RMS as measured with an AFM. The roughness was caused by both roughness in the Bosch DRIE step and line-edge roughness in the mask. In order to reduce the roughness, the grating was polished via KOH to reduce the sidewall roughness. See Figure 7 for an SEM image showing the roughness on the sidewall of a freestanding grating. The polishing process is very delicate and more details can be found by Bruccoleri et al.[2,3] The key idea for KOH polishing is to start with a <110> wafer and align the grating bars to the {111} planes. KOH etches the non-{111} planes approximately 100 times faster than the {111} planes,[21] which means the grating can be etched to remove roughness for long durations without destroying the structure. This requires precise (0.2°) alignment to the {111} planes.

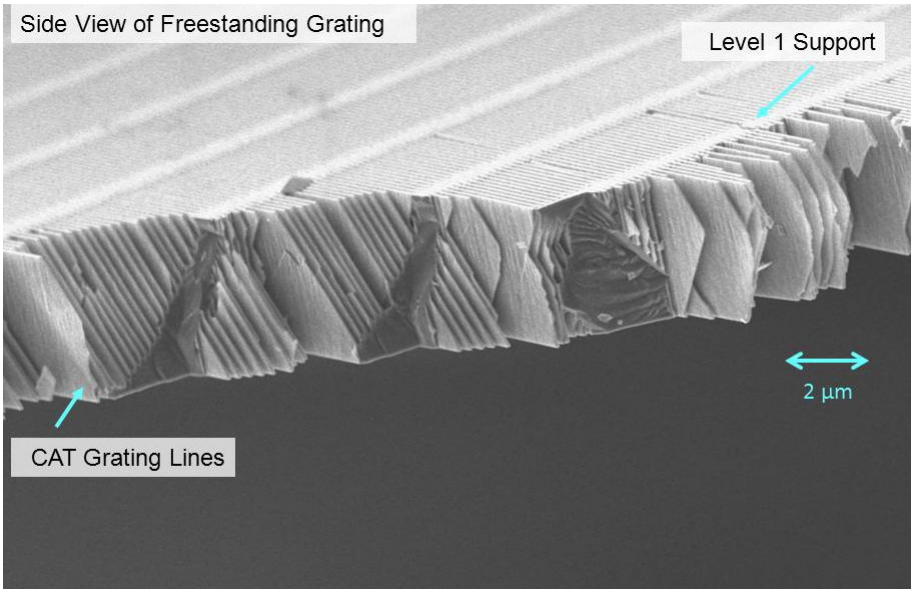

(a)

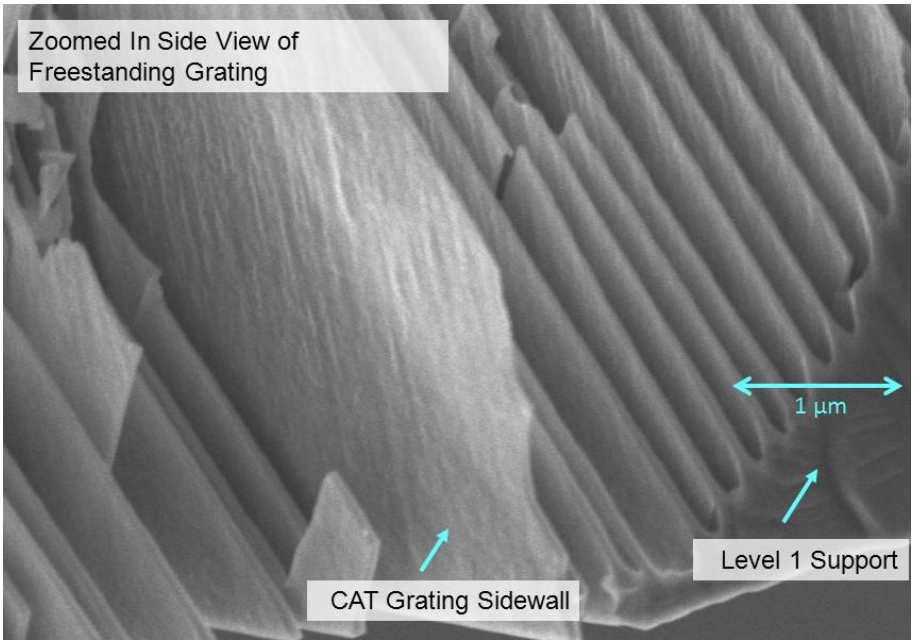

(b)

Figure 7: Slanted SEMs of torn freestanding CAT grating film. The roughness in the CAT grating sidewalls can be observed. (a) Freestanding grating. (b.) Zoomed in on rough sidewall

In order to accomplish this, a wagon wheel with channel-widths of 6 μm, spokes increments of 0.05°, spanning $\pm 3°$ is patterned on the edge of the wafer to within $\pm 1°$ of the major flat at the beginning of the fabrication process. In addition to patterning the wagon wheel, a 5 μm-period grating patch spanning approximately 2 mm is patterned parallel to the zeroth spoke of the wagon wheel. Both the wagon wheel and grating patch are patterned together via contact lithography from a single mask. This grating patch is etched into the silicon and is protected through the subsequent fabrication steps via Kapton tape. The wagon wheel is immersed in 50% KOH by weight for approximately 24 hours and the majority of the misaligned spokes are laterally etched away. The midpoint of the remaining spokes represents the minimum lateral etch rate and the orientation of the {111}

planes relative to the grating patch lines. An array of diffraction orders is created via this grating patch, from each arm of the Mach-Zehnder interference lithography table used to pattern the 200 nm-period CAT grating lines.[19] The array of diffraction orders from the 5 μm-period grating patch rotate as the wafer is rotated, and when the two arrays are parallel, the two incident arms of the Mach-Zehnder are at the same angle relative to the grating patch lines. The 200 nm-period standing waves (image grating) are now parallel to the grating patch lines. Finally, the wafer can be rotated on a vernier chuck by the amount determined via the KOH etch of the wagon wheel, to align the 200 nm-period image grating to the {111} planes. The 200 nm-pitch CAT grating lines are then exposed and developed.

The CAT grating pattern is transferred into the mask and then deep-etched into silicon. An improved front side process was created to increase the minimum bar-width. This was necessary since prior deep etches had a mininum bar width of approximately 50 nm and insufficient silicon remained between two {111} planes to enable successful polishing. See Figure 8 for SEM images of the improved DRIE process. The samples undergo a four-step clean after DRIE: piranha to remove the majority of the organic contamination, CR-7 to remove chrome (if chrome is used in the masking process), $\sim$ 100 ml 3M Novec 7200 ($C_4F_9OC_2H_5$,)[22] on a hot plate set for 200° C for 10 minutes to remove the Bosch process polymer and 50:1 DI water:HF for 60 seconds to remove native SiO_2. Following the clean step, the samples are polished in 50% KOH by weight at room temperature and rinsed in DI water for times ranging between 20 and 43 minutes. The grating is fragile after polishing and it must be critical-point dried to avoid damage from liquid-air surface tension forces. See Figure 9 for SEM images of the polished grating in bulk <110> silicon.

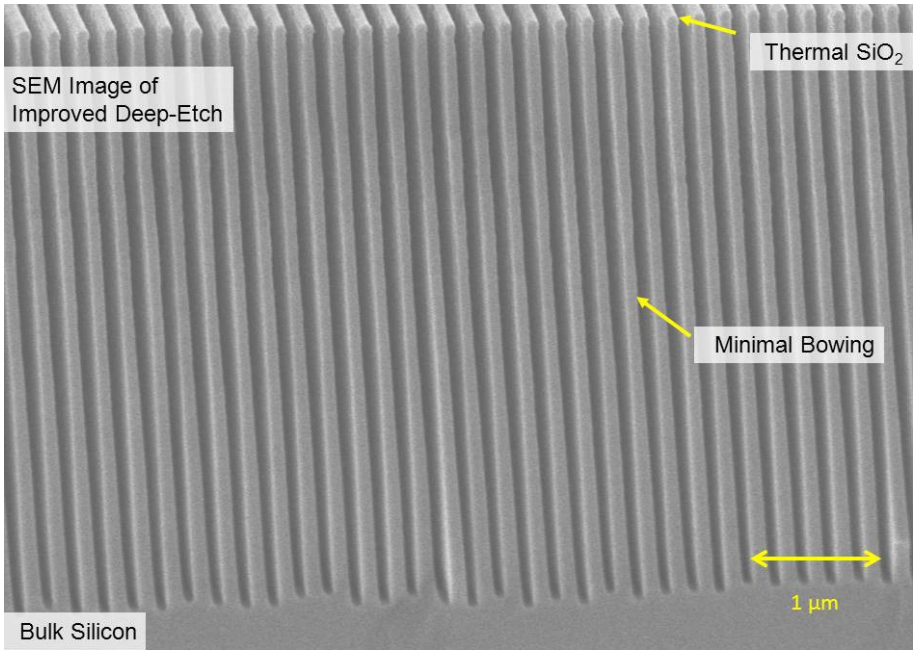

(a)

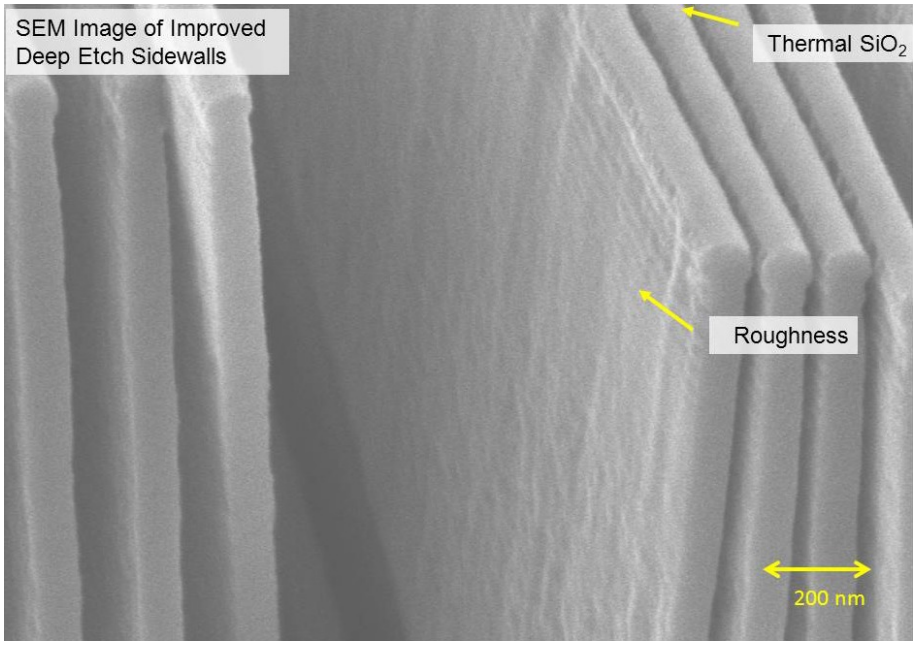

(b)

Figure 8: Cross section SEMs of the improved deep-etch process. This sample was etched for 9 minutes 30 seconds and was not used for later polishing experiments. A sidewall was observed to show roughness. (a.) Zoomed out (b.) Zoomed in sidewall

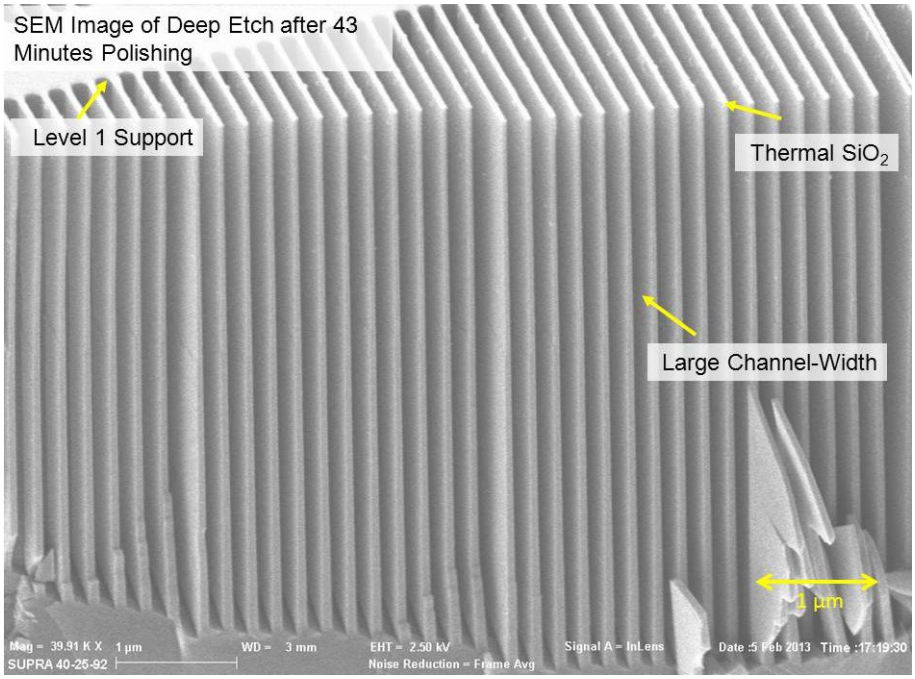

(a)

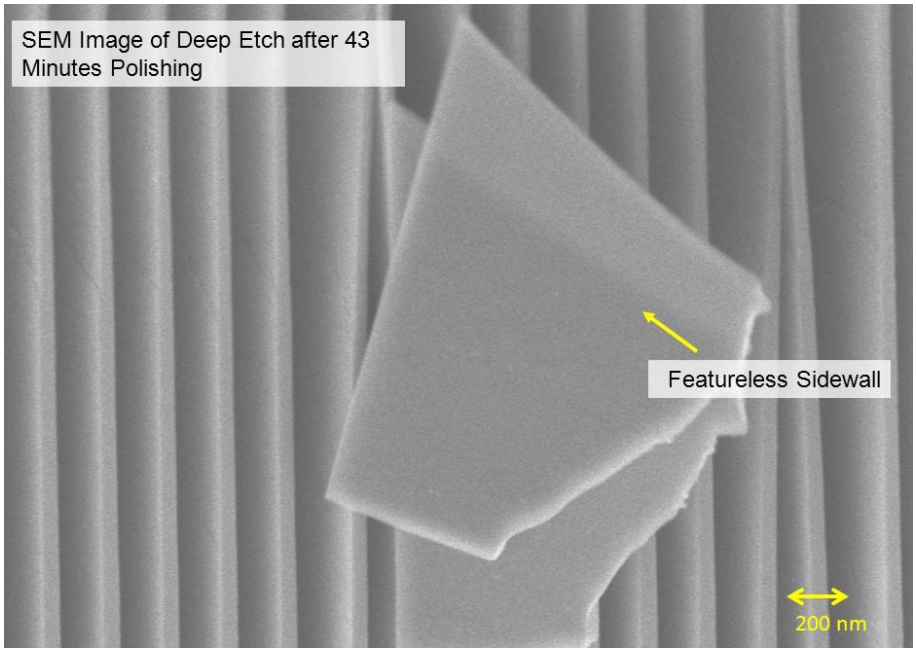

(b)

Figure 9: Cross section SEMs of polished 200 nm-period, 4 μm deep gratings. A sidewall was observed to show improved smoothness. (a.) Zoomed out (b.) Zoomed in

2.3 Polished Freestanding Grating

This polishing process has been demonstrated for <110> silicon wafers, and the current challenge is to integrate polishing into the process for the freestanding grating. This introduces several challenges since polished grating lines become significantly more fragile. The polishing process itself is also delicate and damage during processing could prevent a successful polish. There are two opportunities to polish; either after the front side DRIE step

prior to filling and protecting (after step 3 in Figure 2) or at the end of the process after the back side DRIE. If polishing occurs at the end of the process, the buried SiO_2 would be removed after polishing instead of at step 6, to avoid KOH from etching the grating bars from the bottom.

The experimental work has focused on polishing after DRIE and a freestanding grating has successfully been fabricated; however, the tops of the grating bars are bent requiring further process refinement. The sample was cleaned and polished after DRIE for 30 minutes. It was then filled and protected with photoresist and carried through the process outlined for a freestanding grating. The grating film survived the process unfortunately the tops of the grating bars were bent and often stuck together. See Figure 10 for SEM images of the freestanding polished grating. They were thin at the top, less than 30 nm, and approximately 100 nm at the bottom which suggest the KOH etched the top faster than the bottom. It is also possible the sample was exposed to an air-liquid interface during processing and surface tension damaged the grating bars. Further experiments will be carried out to isolate the cause of the damage. A gentler filling step may be required as well to prevent damage to the grating bars which are twice as thin post polishing.

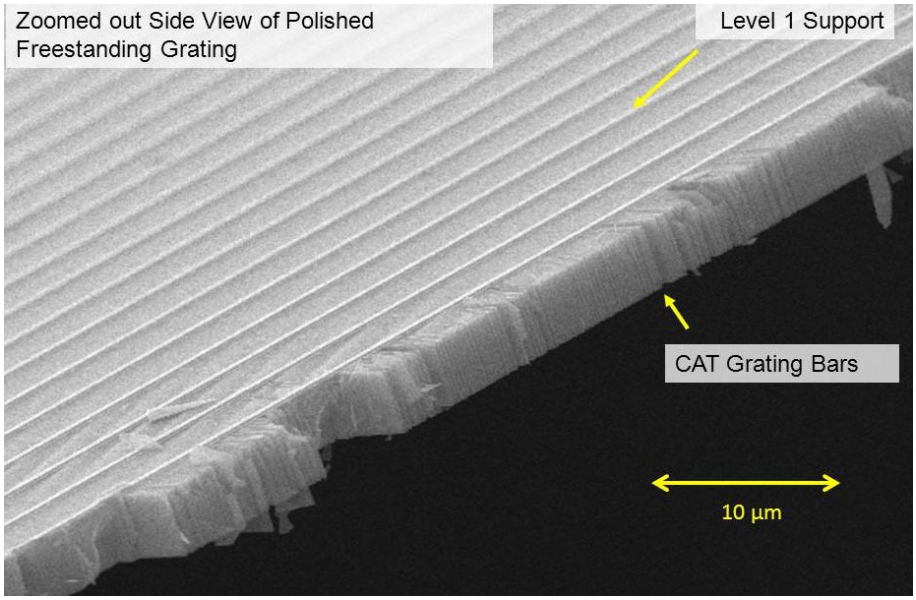

(a)

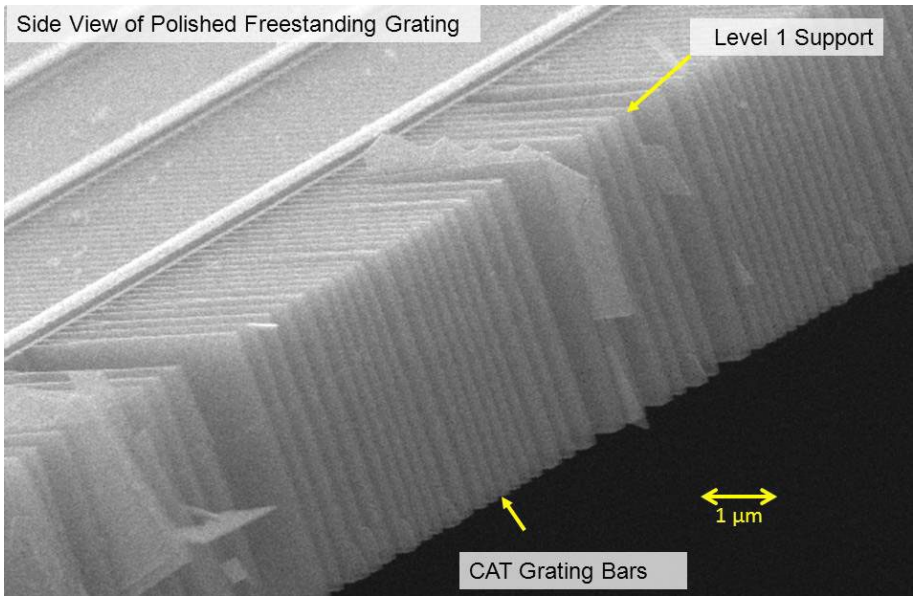

(b)

Figure 10

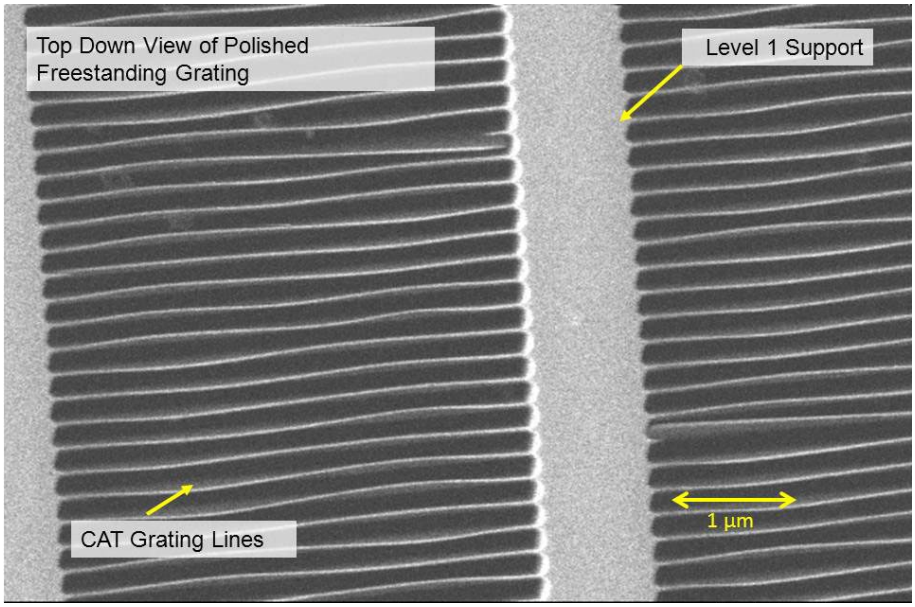

(c)

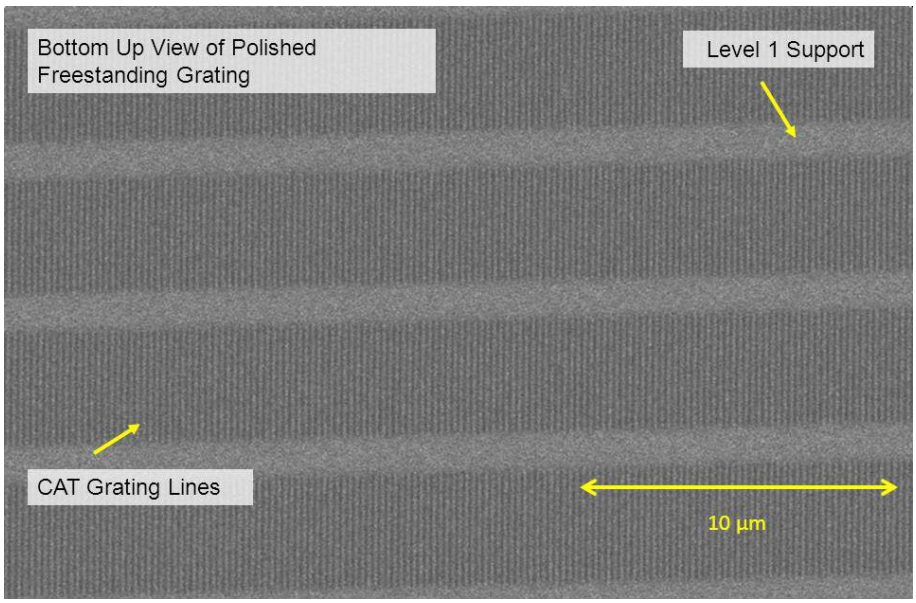

(d)

Figure 10: SEMs of freestanding polished CAT grating. (a.) and (b.) Zoomed out and zoomed in, slanted images of torn freestanding CAT grating film. (c.) Top down image of grating film. (d.) Bottom up image of grating film.

3. CONCLUSION

Multiple nanofabrication processes are presented to create a CAT grating capable of undergoing testing with x-ray sources to demonstrate resolution and diffraction efficiency. The first process created a freestanding grating with unpolished sidewalls, a structure capable of undergoing structural tests. A successful process for polishing CAT grating bars in bulk <110> silicon via KOH is also presented. A combination of those two processes has been presented to fabricate polished freestanding CAT gratings. The process is still in refinement as the grating bars are too thin and bent at the top when the process is completed. Future experiments will be conducted to

improve the understanding of the combined polishing and filling process. Modifications will be made to reduce damage to the grating bars and improve structural rigidity for the subsequent fabrication steps. Furthermore polishing after the back side DRIE step will be explored if the filling process cannot be modified to prevent damaging the grating.

ACKNOWLEDGMENTS

This work was funded by NASA grants NNX11AF30G and NNX12AF21G, the MIT Kavli Institute and the Department of Defense National Defense Science and Engineering Graduate (NDSEG) fellowship program. Specific thanks to James Daley of the MIT Nanostructures Lab, Vicky Diadiuk, Dennis Ward, Dave Terry and Paul Tierney of the Microsystems Technology Laboratories, and Brian VanDerElzen of the University of Michigan Lurie Nanofabrication Facility.

REFERENCES

[1] Bruccoleri, A., Mukherjee, P., Heilmann, R. K., Yam, J., Schattenburg, M. L., and DiPiazza, F., "Fabrication of nanoscale, high throughput, high aspect ratio freestanding gratings," *Journal of Vacuum Science & Technology B: Microelectronics and Nanometer Structures* **30**(6), 06FF03–06FF03–5 (2012).

[2] Bruccoleri, A., *Fabrication of High-Throughput Critical-Angle X-ray Transmission Gratings for Wavelength-Dispersive Spectroscopy*, doctoral thesis, Massachusetts Institute of Technology, Department of Aeronautics and Astronautics (June 2013).

[3] Bruccoleri, A., Guan, D., Mukherjee, P., Heilmann, R. K., Vargo, S., and Schattenburg, M. L., "Potassium hydroxide polishing of nanoscale deep reactive-ion etched ultra-high aspect ratio gratings," *Accepted for publication in Journal of Vacuum Science & Technology B: Microelectronics and Nanometer Structures* (2013).

[4] Heilmann, R. K., Davis, J. E., Dewey, D., Bautz, M. W., Foster, R., Bruccoleri, A., Mukherjee, P., Robinson, D., Huenemoerder, D. P., Marshall, H. L., Schattenburg, M. L., Schulz, N. S., Guo, L. J., Kaplan, A. F., and Schweikart, R. B., "Critical-angle transmission grating spectrometer for high-resolution soft x-ray spectroscopy on the International X-ray Observatory," in [*Proc. SPIE*], **7732**, 77321J (July 2010).

[5] van Beek, J. T. M., Fleming, R. C., Hindle, P. S., Prentiss, J. D., Schattenburg, M. L., and Ritzau, S., "Nanoscale freestanding gratings for ultraviolet blocking filters," *Journal of Vacuum Science & Technology B: Microelectronics and Nanometer Structures* **16**, 3911–3916 (Nov. 1998).

[6] David, C., Bruder, J., Rohbeck, T., Grunzweig, C., Kottler, C., Diaz, A., Bunk, O., and Pfeiffer, F., "Fabrication of diffraction gratings for hard x-ray phase contrast imaging," *Microelectronic Engineering* **84**(5-8), 1172–1177 (2007).

[7] Keith, D. W., Schattenburg, M. L., Smith, H. I., and Pritchard, D. E., "Diffraction of atoms by a transmission grating," *Physical Review Letters* **61**, 1580–1583 (Oct 1988).

[8] Canizares, C. R., Schattenburg, M. L., and Smith, H. I., "The high energy transmission grating spectrometer for AXAF," in [*Proc. SPIE*], **597**, 253–260 (1986).

[9] Paerels, F., "X-ray diffraction gratings for astrophysics," *Space Science Reviews* **157**(1-4), 15–24 (2010).

[10] Heilmann, R. K., Ahn, M., and Schattenburg, M. L., "Fabrication and performance of blazed transmission gratings for x-ray astronomy," in [*Society of Photo-Optical Instrumentation Engineers (SPIE) Conference Series*], *Society of Photo-Optical Instrumentation Engineers (SPIE) Conference Series* **7011**, 701106–701106–10 (Aug. 2008).

[11] Spiller, E., [*Soft X-ray optics*], SPIE Optical Engineering Press, Bellingham, WA, (1994).

[12] Bookbinder, J. A., Smith, R. K., Bandler, S., Garcia, M., Hornschemeier, A., Petre, R., and Ptak, A., "The Advanced X-ray Spectroscopic Imaging Observatory (AXSIO)," in [*Society of Photo-Optical Instrumentation Engineers (SPIE) Conference Series*], *Society of Photo-Optical Instrumentation Engineers (SPIE) Conference Series* **8443**, 844317–844317–7 (Sept. 2012).

[13] Vikhlinin, A., Reid, P., Tananbaum, H., Schwartz, D. A., Forman, W. R., Jones, C., Bookbinder, J., Cotroneo, V., Trolier-McKinstry, S., Burrows, D., Bautz, M. W., Heilmann, R., Davis, J., Bandler, S. R., Weisskopf, M. C., and Murray, S. S., "SMART-X: Square Meter Arcsecond Resolution x-ray Telescope," in [*Society of Photo-Optical Instrumentation Engineers (SPIE) Conference Series*], *Society of Photo-Optical Instrumentation Engineers (SPIE) Conference Series* **8443**, 844316–844316–11 (Sept. 2012).

[14] Mukherjee, P., Zurbuchen, T. H., and Jay Guo, L., "Fabrication and testing of freestanding Si nanogratings for UV filtration on space-based particle sensors," *Nanotechnology* **20**, 325301 (Aug. 2009).

[15] Kovacs, G. T. A., Maluf, N. I., and Petersen, K. E., "Bulk micromachining of silicon," *Proc. IEEE* **86**(8), 1536–1551 (1998).

[16] Jeong, D.-H., Yun, S.-S., Lee, M.-L., Hwang, G., Choi, C.-A., and Lee, J.-H., "Novel micro capacitive inclinometer with oblique comb electrode and suspension spring aligned parallel to {111} vertical planes of (110) silicon," in [*Micro Electro Mechanical Systems, 2009. MEMS 2009. IEEE 22nd International Conference on*], 797–800 (Jan.).

[17] Jeong, D.-H., Yun, S.-S., Lee, B.-G., Lee, M.-L., Choi, C.-A., and Lee, J.-H., "High-resolution capacitive microinclinometer with oblique comb electrodes using (110) silicon," *Microelectromechanical Systems, Journal of* **20**(6), 1269–1276 (Dec.).

[18] Mukherjee, P., Bruccoleri, A., Heilmann, R. K., Schattenburg, M. L., Kaplan, A., and Guo, L., "Plasma etch fabrication of 60:1 aspect ratio silicon nanogratings with 200 nm pitch," *Journal of Vacuum Science & Technology B: Microelectronics and Nanometer Structures* **28**(6), C6P70–C6P75 (2010).

[19] Schattenburg, M. L., Anderson, E. H., and Smith, H. I., "X-ray/VUV transmission gratings for astrophysical and laboratory applications," *Physica Scripta* **41**, 13–20 (Jan. 1990).

[20] Schattenburg, M. L., "From nanometers to gigaparsecs: The role of nanostructures in unraveling the mysteries of the cosmos," *Journal of Vacuum Science & Technology B: Microelectronics and Nanometer Structures* **19**, 2319–2328 (Nov. 2001).

[21] Ahn, M., *Fabrication of critical-angle transmission gratings for high efficiency x-ray spectroscopy*, doctoral thesis, Massachusetts Institute of Technology, Department of Mechanical Engineering (February 2009).

[22] Clark, P. G., Olson, E. D., and Kofuse, H., "The Use of Segregated Hydrofluoroethers as Cleaning Agents in Electronic Packaging Applications," *International Conference on Soldering and Reliability, Toronto, Ontario, Canada* (May 2009).